J Ther Eng, Vol. 9, No. 3, pp. 786−798, May, 2023

Journal of Thermal Engineering
Web page info: https://jten.yildiz.edu.tr
DOI: 10.18186/thermal.1300835

Journal of Thermal Engineering

Research Article

Thermodynamic analysis of the apci skikda liquefaction process

Chaima DERBAL[1,*], Abdallah HAOUAM[1]

[1]*Department of Mechanical Engineering, Faculty of Technology, Industrial Mechanics Laboratory, Badji Mokhtar University, Annaba, 23000 Algeria*

ARTICLE INFO

Article history
Received: 06 April 2022
Revised: 13 June 2022
Accepted: 17 June 2022

Keywords:
APCI; LNG; Mixed Refrigerant; COP; Exergy Efficiency; Optimization; Genetic Algorithm

ABSTRACT

In this paper, the mixed refrigeration cycle of Skikda APCI (Air Products and Chemicals Inc.) process in Algeria was studied thermodynamically in order to determine the optimal operating conditions. The energy and exergy balance equations for each process component were established. The distribution of the exergy destruction of the basic cycle equipment revealed that the compressors had the highest exergy destruction rate. The effects of operating conditions on performance coefficient of the cycle (COP) and exergy efficiency of the APCI process were evaluated; mainly the inlet temperature of the compressors, natural gas (NG) temperature after cooling in the main cryogenic heat exchanger (MCHE) and inlet temperature of the mixed refrigerant (MR) expansion valve. The results of the numerical simulation validated using Aspen HYSYS software indicate that the COP and exergy efficiency of the basic cycle are 2.66 and 59.99% respectively. These results can be improved by reducing the inlet temperature of the compressor and the expander as well as that of the NG after cooling in the MCHE. Finally, the results of the optimization performed using the genetic algorithms (GA) are in agreement with those of the literature. They show signs of improvement in the COP and exergy efficiency of the APCI process by 1.48% and 3.64% respectively compared to the basic cycle.

Cite this article as: Derbal C, Haouam A. Thermodynamic analysis of the apci skikda liquefaction process. J Ther Eng 2023;9(3):786−798.

INTRODUCTION

Today, liquefied natural gas (LNG) is considered one of the most important energy carriers. It is produced by three cryogenic gas liquefaction processes: cascade cycles with pure refrigerants, mixed refrigerant cycles and nitrogen expansion cycles. Mixed refrigerant processes are mainly divided into three types: single mixed refrigerant (SMR), dual mixed refrigerant (DMR) and cascaded mixed refrigerant cycles [1]. Among these mixed refrigerant processes, the APCI-LNG process is the most widespread in the cryogenic industry, currently belongs to the majority of liquefaction plants in the international market, accounts for about 40% of the capital of LNG complexes and has a significant impact on utilities and operating costs.

Many researchers have been conducting theoretical and experimental studies and have been interested to the optimization of this liquefaction process for more than three decades.

Kikkawa et al. [2] simulated a uniform refrigerant liquefaction process using a pre-cooling loop and an expander

*Corresponding author.
*E-mail address: chaim.23.derb@gmail.com

This paper was recommended for publication in revised form by Regional Editor Ahmet Selim Dalkılıç

with the CHEMCAD III software. Process thermal efficiency has been evaluated based on the required power consumption to produce a unit of LNG, i.e., specific power consumption. The total required power consumption of the refrigerant compressors is 81.5MW which is equivalent to a specific power of 931 kJ/kg of LNG. Cao et al. [3] designed and simulated two types of small-scale NG liquefaction processes in a skid-mounted assembly, their results show that the N_2-CH_4 expansion cycle precedes the mixed refrigeration cycle due to the absence of propane pre-cooling. The power consumption of the compressors is more influential to specific power consumption, so compression with intercooling should be adopted to lessen the irreversible degree of compression process. Vatani et al. [4] considered two mixed refrigeration cycles for the design of an LNG production process with integrated natural gas liquids recovery. They formulated an optimization problem with minimization of specific energy consumption. Their results showed that not only liquefaction efficiency of the process is considerable (0.414 kWh/kg LNG) but also it can recover the ethane higher than 93.3%. This process can be used for large LNG plants in the natural gas refineries. It can also be said that the overall efficiency will be higher for the leaner feed gases. Wang et al. [5] optimized two types of C3MR processes by studying different objective functions, including shaft work consumption, exergy efficiency and operating expenses. They reported that tree work consumption is the best objective function for the optimization of these processes. Khan and Le [6] optimized SMR and C3MR processes using knowledge based optimization (KBO) method. By considering boiling point difference of the MR components, they improved the energy efficiency of the system. They reduced the compression energy requirement of an SMR process by 10% with warm particles model, while the exergy efficiency of the whole process increases 5%.

Kumar and Mishra [7] presented a detailed review for cryogenic systems and made energy and exergy analysis of the system for liquefaction of various gases. Mehrpooya and Ansarinasab [8] conducted an energy and exergy analysis for the Linde SMR and APCI single mixed refrigeration processes. Their results show that the exergy efficiency and exergy destruction rate of the APCI process are 45% and 72.24MW respectively. Derbal al. [9] made an exergy analysis of the mixed refrigeration APCI-LNG Skikda and determined exergy efficiency and exergy destruction of the MR compressors and gas turbine. Their results show that the inlet temperature and inlet pressure of MR compressors has an impact on the evolution of the exergy efficiency. Wang et al. [10] experimentally investigated the effect of operating pressures and refrigerant flow compositions on the cycle performance; they concluded that the openings of two throttle valves had significant impacts on operating pressures.

Hajji et al. [11] performed simulation and sensitivity analysis for two objective functions, specific energy and compressor energy consumption, by the Aspen HYSYS process simulator and this was done to improve the overall performance and heat recovery of the LNG process output streams by changing the thermodynamic variables of the C3MR mixed refrigerant process. The results obtained show a greater improvement in the objective functions compared to other studies. He et al. [12] proposed a simulation-based optimization methodology to simultaneously determine the components and their respective fractions in the MR. Then; they performed energy and exergy analysis to reveal the relationships between the MR components and the process performance. Their results indicated that energy efficiency and exergy efficiency were strongly influenced by the selection of components for the MR. Aghazadeh et al. [13] carried out a comprehensive thermodynamic analysis and optimization of two new combined refrigeration cycles using the first and second thermodynamic laws and the assumption of a constant area model for the ejector. Their results show that the maximum thermal efficiency and exergy efficiency are 77.3% and 23.7% in cycle I and 87.5% and 23.9% in cycle II, respectively, by optimizing all design parameters. Rehman et al. [14] presented a systematic approach that includes the identification of improvement potentials in the single mixed refrigeration process SMR. To this end, sources of irreversibility are identified using an advanced exergy analysis to identify further improvement potential. The results reveal that 43% of the overall energy destruction associated with the base case of the SMR process can be avoided through process optimization or redesign.

Genetic algorithm (GA) is a global optimization method applied for optimizing LNG process. Alabdulkarem et al. [15] applied GA for the optimization of the propane precooled mixed refrigeration cycle and reported the energy consumption of the MR at different compression pinch temperatures using a combination of GA and sequential quadratic programming. Xu et al. [16] modeled and optimized the PRICO process using GA and Aspen Plus software; the result shows that at about the 40th generation, the search identifies the optimal solution. They obtained a relationship between energy consumption and mixed refrigerant composition. Moein et al. [17] analyzed a single mixed refrigeration cycle (SMR) to determine the optimal operating conditions and optimized it with using GA. They minimized the total required work by optimizing eleven variables including the outlet pressures of all compressors and throttling valves and the molar flow rate of the MR components. The results showed that the total required work was reduced by 14% compared to the base case. Nikkho et al. [18] carried out a simulation of two small-scale modified single refrigeration processes for NG liquefaction. They used the GA method to optimize the specific energy consumption and the total exergy destruction rate of the process. Their results show that the specific energy consumption and the total exergy destruction rate are reduced by 19.4% and 25.4%, respectively. On the other

hand, the maximum total exergy efficiency of 47.51 % is obtained.

The literature review shows that the APCI cycle is the most efficient for the production of LNG. In this context, fits our contribution. The objective of our work is to determine the efficiency of the APCI Skikda (Algeria) liquefaction process, compare it to other liquefaction processes and seek its improvement. To do so, this cycle will be thermodynamically analyzed. The energy analysis will lead to obtaining the COP of the cycle while the exergy analysis will allow the detection of irreversibilities within the process equipment and the evaluation of the exergy efficiency of the cycle. The effects of important parameters (compressor inlet gas temperature, expander inlet temperature and MCHE outlet temperature) on APCI process performance will be studied and the main results will be described. The genetic algorithm will be used as a method of performance optimization. The optimization results are described and compared to those of the literature. The details of this work are represented in the following sections.

APCI Process Description

The APCI process used in Skikda LNG complex includes three refrigeration cycles (mixed refrigeration, propane refrigeration and external propane refrigeration). In this descriptive section, we limit ourselves to the mixed refrigeration cycle, subject of this work. It is mainly composed of a main cryogenic heat exchanger (MCHE), three compressors (C1, C2 and C3) and chillers (c4-c5-...-c11). The process is shown in Figure. 1. The NG flows through the HP, MP, BP propane feed gas coolers (c1, c2 and c3) at (22.46°C, 63 bar). The NG coming from the c3 cooler enters the scrubber column (SC) (Stream 4) at (-35.15°C, 61.56 bar). The head stream of the SC feeds the hot end of the MCHE at (-38.99°C, 60.67 bar) (Stream 6) and then returns to the reflux drum (RD) at -55.33°C of the SC via

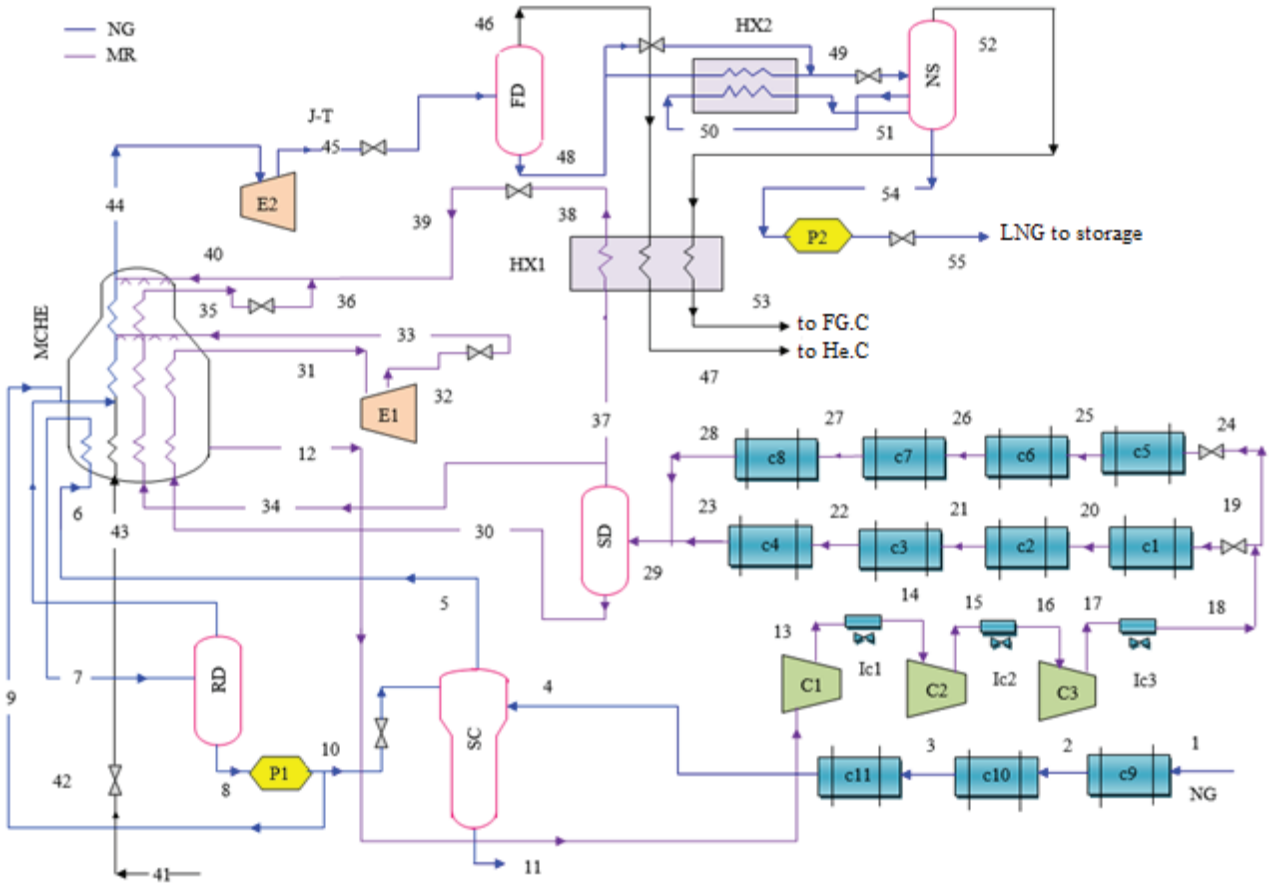

Legend

E Expander c1-... c3 Gas cooler JT Thomson Joule valve *RD* Reflux Drum
FD Flash Drum C1-…C3 Compressor P1, P2 Pump *SD* Separator Drum
HX Heat exchanger c4-…c11 Chiller NS Nitrogen Stripper *SC* scrub column
He.C Helium Compressor Ic1-…Ic3 Intercooler MCHE Main Cryogenic Heat Exchanger
FG.C Fuel Gas Compressor

Figure 1. Schematic diagram of the APCI - Skikda liquefaction process.

Table 1. Chemical composition of NG and MR

Components	Mole fraction (%) NG	Mole fraction (%) MR
He	0.19	-
N_2	5.78	5.22
CH_4	82.49	48.90
C_2H_6	7.27	37.15
C_3H_8	2.35	8.73
i-C_4H_{10}	0.47	-
n- C_4H_{10}	0.68	-
i-C_5H_{12}	0.15	-
n-C_5H_{12}	0.19	-
C_6H_{14} (C^{+6})	0.23	-
CO_2	0.21	-
H_2O	0.01	-

pump P1. Streams (12) to (40) constitute the MR loop. The mixed refrigeration system recovers the MR as steam from the shell side of the MCHE at -39.17°C (Stream 12). The MR discharged by compressors (C1, C2) is cooled in intercoolers (Ic1, Ic2) before being sent to the compressor suction (C3). After discharge from the compressor (C3), the MR is cooled in the intercooler (Ic3) to 40.76°C (Stream 18). The coolers (c4-...-c11) cool the MR from 40.76°C to -35.69°C before it enters the MCHE (Stream 30). The MR liquid leaving the MCHE mid-tip (Stream 31) is expanded by the E1 expander from 49.66 bar to 4.7 bar and returns to the exchanger through the Thomson Joule valve (Stream 33). The LNG expander E2 receives the liquefied natural gas from the cold end of the MCHE (Stream 44) at a pressure of 45.85 bar and expands it to a pressure of 21.79 bar (Stream 45) before it is admitted into the flash drum (FD) (Stream 46). The MR refrigerant from the separator (SD) feeds the exchanger (HX1) at -35.69°C (Stream 37). The head product from the flash drum (FD) enters the exchanger (HX1) at -147.77°C (Stream 46) to feed the helium compressor (He.C) (Stream 47) at -37.91°C The exchanger (HX2) receives the hot LNG from the bottom of the flash drum (FD) at -147.77°C (Stream 48). The LNG product at -160.55°C coming from the bottom of the nitrogen stripper (NS) (Stream 54) is sent to the LNG storage tank thanks to the P2 pump (Stream 55).

The chemical composition of NG and MR are shown in Table 1.

THERMODYNAMIC ANALYSIS

In order to analyze the performance of the system, the influence of the inlet temperature of the compressors, the inlet temperature of the expander, the temperature of the NG after cooling in the MCHE, on the COP and the exergy efficiency of the APCI cycle has been evaluated in this study. The thermodynamic analysis is based on a numerical simulation performed with the Matlab® program. The energy equilibrium equations and the exergy equilibrium equations of the APCI cycle equipment are established by neglecting the pressure loss and the heat loss in the heat exchangers. This analysis was carried out on the basis of the assumptions presented in Table 2.

Table 2. Main assumptions for the thermodynamic analysis of the basic cycle

Parameter	Value
NG source inlet temperature, °C	22.46
NG source inlet pressure, bar	63
NG mass flow rate, kg/s	233.39
MR mass flow rate, kg/s	359.039
LNG mass flow rate, kg/s	205.96
Expander isentropic efficiency	0.87
Compressor isentropic efficiency	0.87
Ambient temperature, °C	25
Ambient pressure, bar	1.013

Energy Analysis

The steady-state energy balance equation is expressed as:

$$\sum_{k=1}^{n} \dot{m}_k \left(\frac{v_k^2}{2} + g z_k + h_k \right) + \dot{Q} - \dot{W} = 0 \qquad (1)$$

Neglecting the kinetic and potential energy variations ($\frac{v_k^2}{2}$ and gz_k), the energy balance equations for each component can be written in terms of specific enthalpy as follows [19]:

$$\sum \dot{m}_{in} h_{in} - \sum \dot{m}_{out} h_{out} - \dot{W} + \dot{Q} = 0 \qquad (2)$$

For compressors C1, C2 and C3, the energy equation is:

$$\dot{W}_i = \dot{m}_{i,in}(h_{i,out} - h_{i,in}) = \frac{\dot{m}_{i,in}(h'_{i,out} - h_{i,in})}{\eta_c} \qquad (3)$$

i=C1, C2, C3

where $h'_{i,out}$ is the enthalpy at entropy constant and η_c the compressor isentropic efficiency.

For the expander, the energy equation is:

$$\dot{W}_j = \dot{m}_{j,in}(h_{j,in} - h_{j,out}) = \eta_j \dot{m}_{j,in}(h_{j,in} - h'_{j,out}) \qquad (4)$$

j=E1, E2

where $h'_{i,out}$ is the enthalpy at entropy constant and η_i the expander isentropic efficiency.

For heat exchangers HX1and HX2, the energy equation is:

$$\dot{m}_h\left(h_{h,in}-h_{h,out}\right)=\dot{m}_c\left(h_{c,out}-h_{c,in}\right) \tag{5}$$

For the MCHE, the energy equation is obtained from Figure 1:

$$\begin{aligned}&\dot{m}_6h_6+\dot{m}_{43}h_{43}+\dot{m}_{34}h_{34}+\dot{m}_{30}h_{30}+\dot{m}_{33}h_{33}+\\&\dot{m}_{40}h_{40}+\dot{m}_9h_9=\dot{m}_7h_7+\dot{m}_{44}h_{44}+\dot{m}_{31}h_{31}+\dot{m}_{35}h_{35}\end{aligned} \tag{6}$$

The cycle performance coefficient is expressed as:

$$COP=\frac{\dot{Q}}{\dot{W}_{net}}=\frac{\dot{m}_{NG}\left(h_1-h_4\right)+\dot{m}_{LNG}\left(h_9-h_{44}\right)+\dot{m}_{19}\left(h_{19}-h_{23}\right)+\dot{m}_{24}\left(h_{24}-h_{28}\right)}{\sum\dot{W}_i-\sum\dot{W}_j} \tag{7}$$

i=C1, C2, C3; *j*=E1, E2

The input energy is the net work done on the system for the production of LNG, the output energy is the heat supplied by the refrigerants in the NG cooling stages.

Exergy Analysis

The exergy analysis of a process complements the energy analysis and is used to assess the work potential of the input and output material and heat streams, and to determine the location and magnitude of irreversibility losses. The state-specific exergy is determined from the following equation:

$$\dot{E}_x=\dot{E}_x^k+\dot{E}_x^p+\dot{E}_x^{ch}+\dot{E}_x^{ph} \tag{8}$$

In this study, variations in kinetic and potential exergy have been neglected. By assuming a constant chemical composition of the flows, the chemical exergy term is cancelled out in the exergy balance equations. Therefore, the specific exergy for each arbitrary state can be considered equivalent to the physical exergy. The physical exergy is obtained from the following equation [20]:

$$\dot{E}_x=\dot{E}_x^{ph}=\dot{m}\left[\left(h-h_0\right)-T_0\left(s-s_0\right)\right] \tag{9}$$

where (*s*) and (*h*) are the specific entropy and enthalpy at the conditions specified for the species and the subscript 0 represents the environmental conditions. The general exergy balance can be expressed as a rate as follows [21-23]:

$$\dot{E}_{x,in}=\dot{E}_{x,out}+\Delta\dot{E}_x \tag{10}$$

where $\dot{E}_{x,in}$ is the exergy at the input, $\dot{E}_{x,out}$ is the exergy at the output and $\Delta\dot{E}_x$ is the exergy destruction.

The exergy destruction for each process component is calculated based on the well-known equations summarized as follows in Table 3. The total exergy destruction can be found as the sum of the exergy destruction of each component [24-27]:

Table 3. Formulas used to calculate the exergy destruction of the cycle components

Components	Exergy destruction
Compressor	$\Delta\dot{E}_x=\dot{E}_{x,in}-\dot{E}_{x,out}+\dot{W}_c$
Expander	$\Delta\dot{E}_x=\dot{E}_{x,in}-\dot{E}_{x,out}-\dot{W}_e$
Heat Exchanger	$\Delta\dot{E}_x=\sum\dot{E}_{x,in}-\sum\dot{E}_{x,out}$
Cooler; Valve; Separator	$\Delta\dot{E}_x=\dot{E}_{x,in}-\dot{E}_{x,out}$

The exergy efficiency of the cycle is defined as follows [19]:

$$\eta_{ex}=1-\frac{\text{Total exergy destruction of the cycle}}{\text{Power consumed during the cycle}} \tag{11}$$

The thermodynamic properties, including temperature, pressure, mass flow rate, enthalpy, entropy, exergy and steam fraction "x" at each point in the MR cycle of the APCI process are summarized in Appendix 1.

OPTIMIZATION

The genetic algorithm (GA) is a heuristic search that mimics the process of natural selection and is commonly used to generate useful solutions to optimization problems [28]. The design of the liquefaction process is a highly nonlinear problem with many local optima. To solve the optimization problem, GA is chosen as the optimization method [29-31]. The GA starts working by producing an initialization population. During the optimization, there are several constraints to ensure that the process can run safely and stably. The GA will judge whether the constraints are satisfied or not. If the constraints are satisfied, the GA will calculate the objective function; otherwise, the penalty function will replace the objective function. The best population will be found when the objective function reaches the maximum or minimum value.

The 'Stochastic uniform' method is used as a selection method in this paper, namely it stochastically chooses a number of chromosomes from the current population and selects the one with the best 'fitness'. Breeding is carried out

by the 'Scattered' crossover method. Then chain mutations occur randomly with minor probability and a new individual is finally formed. In order to save the best solution from each generation, the corresponding optimal fitness solution is compulsively copied into the next generation. The parameters used for the GA are presented in Table 4, as for the variables used for the cycle optimization are presented in Table 5.

Table 4. Parameters used in GA

Parameter	Value
Number of population	60
Selection method	Stochastic uniform
Mutation	Uniform
Crossover function	Scattered
Crossover rate	0.85
Migration fraction	0.25
Number of generations	200

Objective Function

In this work, the actual optimization problem is the minimization of the net energy consumption of the APCI cycle. In general, the exergy efficiency of the cycle has been defined as an objective function expressed as follows:

$$f(X) = 1 - \frac{\sum \Delta \dot{E}_x}{\min\left(\dot{W}net\right)} \tag{12}$$

where $\dot{W}_{net}$ indicates the net energy consumption of compression and expansion of the refrigerant and $\sum \Delta \dot{E}_x$ represents the total exergy destruction of the process.

$$\dot{W}_{net} = \sum \dot{W}_{compressors} - \sum \dot{W}_{\exp anders} \tag{13}$$

In Eq. 12, X is an adjusted variable vector including the inlet temperature of the compressors (C1, C2 and C3), the inlet temperature of the expanders (E1, E2).

RESULTS AND DISCUSSION

In this work, energy and exergy analyses were performed on the APCI cycle. Basic cycle performances described under the operating conditions are presented in Table 6. It consumes a net power of about 102.35 MW, while its COP and exergy efficiency are estimated at 2.66 and 59.99% respectively.

Table 6. Results of the thermodynamic calculation of the basic APCI cycle performances

Performance	Value
Expander power E1, MW	1.74
Expander power E2, MW	0.71
Power consumed by C1, MW	57.23
Power consumed by C2, MW	18.53
Power consumed by C3, MW	29.04
Net power input, MW	102.35
Coefficient of performance (COP)	2.66
Exergy destruction, MW	40.95
Exergy efficiency, η_{ex} (%)	59.99

Exergy analysis is applied to assess the extent of exergy destruction in each component of the cycle shown in Figure 2. It is found that compressors occupy the highest proportion of the total exergy destruction rate estimated at 30.43 %, followed by coolers and intercoolers occupying 22.17%. Other important equipments with irreversible operations are the MCHE, expanders, heat exchangers and separators. They contribute respectively with a rate of 19.71%; 8.55%; 7.2% and 7.72% of the total exergy destruction of the liquefaction process. The energy destruction of the throttle valves and pumps are the lowest. Our results are in agreement with the work of the authors [35-38].

It is clear that reducing the exergy destruction in the compressors and coolers would be the best way to reduce the total exergy destruction of this liquefaction process. The main measures to reduce compressor exergy destruction are to adopt multi-stage compression, selecting reasonable inlet parameters and compression ratio for the compressor.

Table 5. Variables limits used for the cycle optimization

Parameter	Basic cycle	Lower bound	Upper bound
C1 Inlet temperature, °C	-39.17	-42	-36
C2 Inlet temperature, °C	34.16	31	37
C3 Inlet temperature, °C	34.72	32	38
E1 Inlet temperature, °C	-128.94 [32-34]	-130	-126
E2 Inlet temperature, °C	-145.94 [32-34]	-146.20	-142

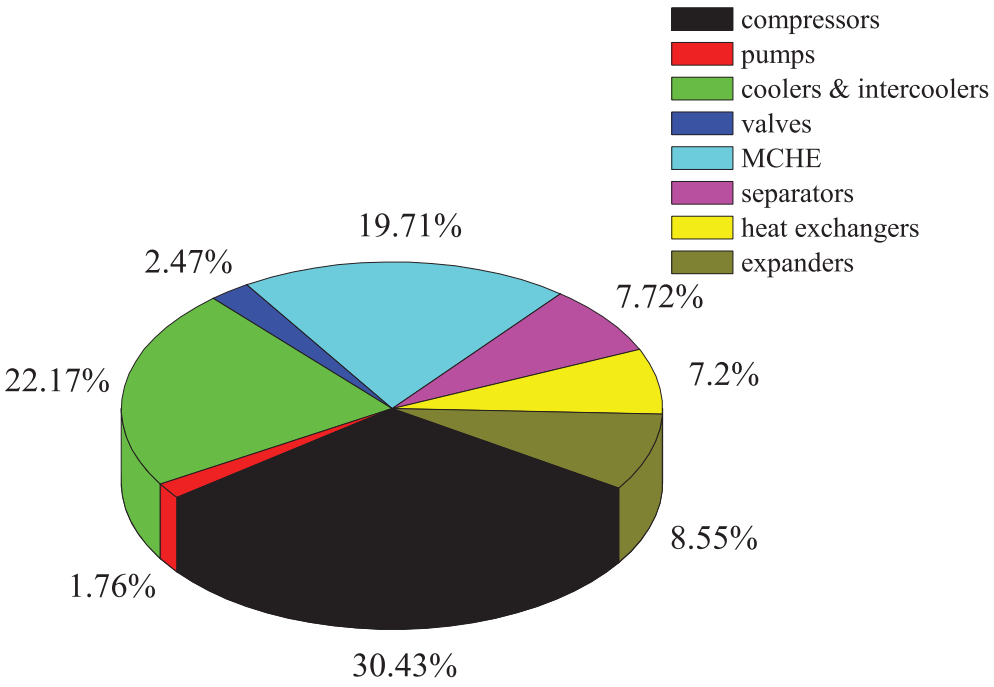

Figure 2. Distribution of exergy destruction rate of the basic cycle components

Thus, the outlet temperature of the compressors is reduced and the heat transfer temperature difference in the coolers is lower. The exergy destruction of the chillers is reduced due to the reduced heat transfer temperature difference.

In this work, the numerical simulation of the key process parameters was carried out using the Aspen HYSYS software. The effects of compressor inlet temperature, NG temperature after cooling in the MCHE and MR expander inlet temperature on the COP and exergy efficiency of the APCI process were analyzed. The results proposed are shown in Figure 3; Figure 4 and Figure 5.

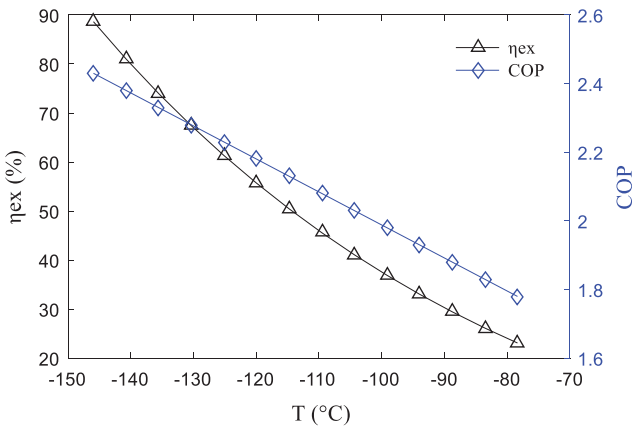

Figure 3. Effect of NG temperature after cooling in MCHE on the COP and exergy efficiency

Figure 3 shows the effects of the NG temperature after cooling in MCHE on the COP and exergy efficiency, where the heat transfer for the NG occurs under a pressure of 45.85 bar. It is seen that increasing the NG temperature after cooling in MCHE induces a decrease in the COP and the exergy efficiency. On the other hand, the increase of the NG outlet temperature after cooling in MCHE induces a reduction of the input power required for the compressors (C1, C2 and C3), the total heat captured from the NG in the MCHE also decreases and finally the COP and exergy efficiency decrease. Figure 3 also shows that at -77°C the COP and exergy efficiency can also reach of about 1.78 and 23.10 %, respectively.

Figure 4 shows the influence of the inlet temperature of the compressors (C1, C2 and C3) on the COP and exergy efficiency, the inlet pressure of the compressors (C1, C2 and C3) is 4.3 bar; 20.61 bar and 31.80 bar respectively. It is seen that the COP and exergy efficiency decrease as the inlet temperature of the compressors (C1, C2 and C3) increases. This is due to the fact that the input power of the compressors increases as the input temperature of the compressors increases. On the other hand, Figure 4 also shows that the COP and exergy efficiency of C1 can also reach about 1.97 and 30.27% respectively; those of C2 about 2.23 and 53.25% respectively; and those of C3 about 2.26 and 63.28% respectively Table 7. Thus, a decrease in compressor inlet temperature would ensure better cycle performances.

The effect of the inlet temperature of the E1 expander on the COP and exergy efficiency is shown in Figure 5 where the inlet pressure of the E1 expander is 49.66 bar. It is seen

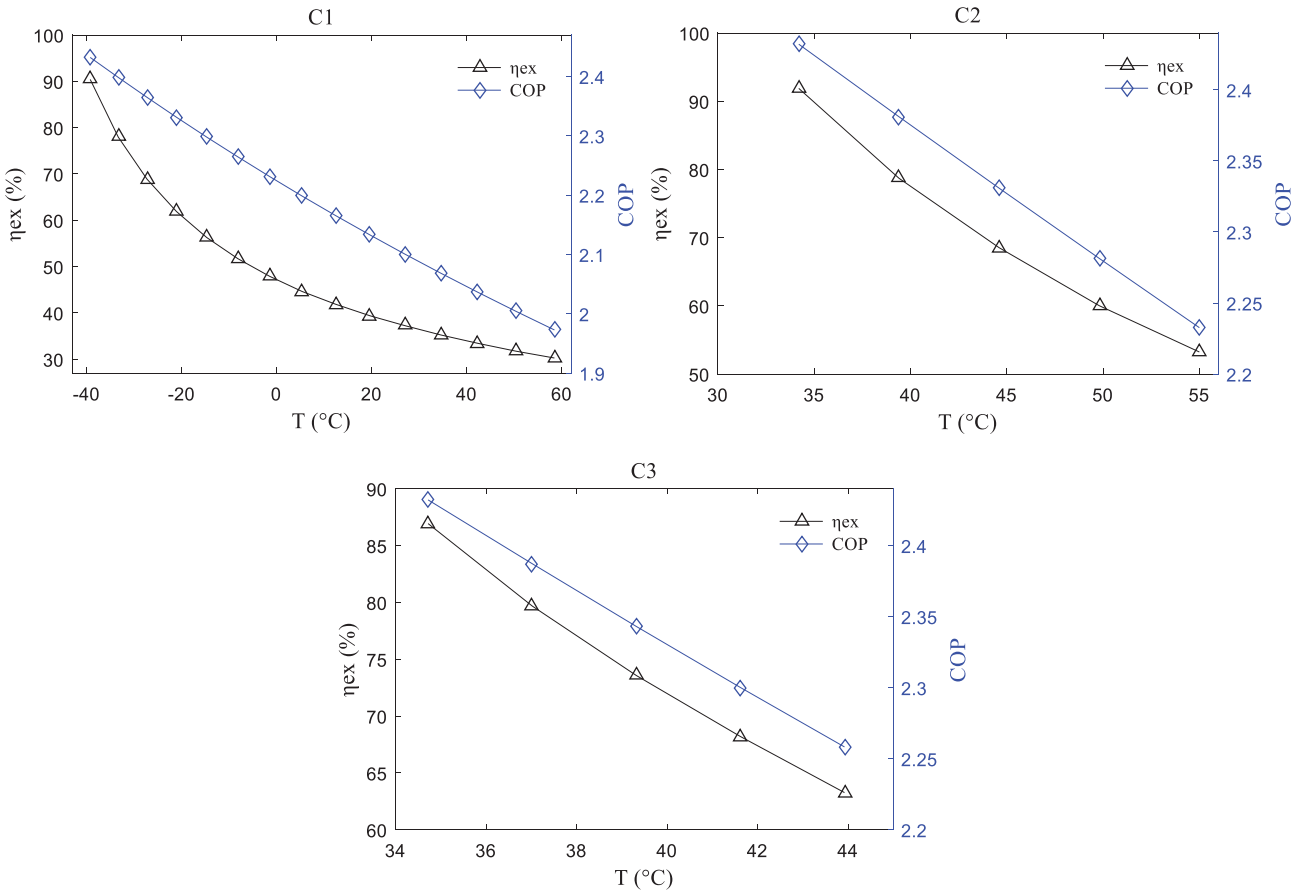

Figure 4. Effect of compressors inlet temperature on the COP and exergy efficiency

Table 7. Cycle performance at maximum compressor inlet temperatures values

Compressor	Inlet P (bar)	Inlet T (°C)	COP	η_{ex} (%)
C1	4.30	58	1.97	30.27
C2	20.11	55	2.23	53.25
C3	31.80	44	2.26	63.28

that the COP and exergy efficiency decrease with increasing inlet temperature of the E1 expander. This decrease is due to the increase in the power of the E1 expander. On the other hand, Figure 5 also shows that the COP and exergy efficiency of the E1 at -112°C can reach 1.84 and 26.33%, respectively. The results commented in Figure 3, Figure 4 and Figure 5 are in accordance with those obtained by the authors [37-38].

To validate simulation results proposed via Aspen HYSYS software, we run the model with basic cycle data as input and adjust it until the output produced matches the basic cycle results. This validation is represented in Table 8.

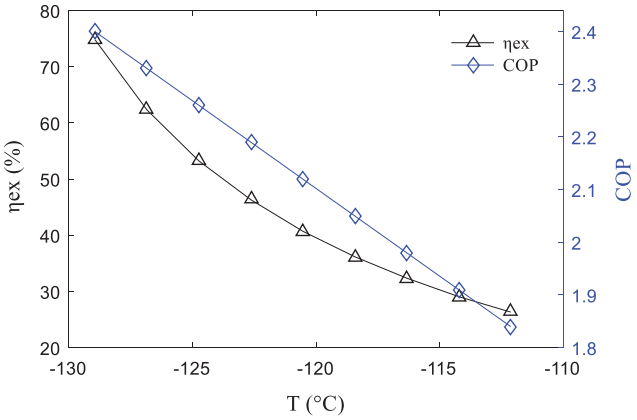

Figure 5. Effect of E1 expander inlet temperature on the COP and exergy efficiency

We note that the differences between the values of the parameters of the basic cycle and those proposed by simulation via HYSYS do not exceed 6.77%, which confirms the validity of our results. The optimization results indicate that the minimum power requirement for the three

Table 8. Validation of the numerical simulation results via Aspen HYSYS

Parameter	Basic cycle	Aspen HYSYS	Deviation (%)
C1 Outlet temperature, °C	62.43	60.11	3.71
C2 Outlet temperature, °C	66.48	65.79	1.04
C3 Outlet temperature, °C	85.88	85.02	1
E1 Outlet temperature, °C	-129.30	-129.6	0.23
E2 Outlet temperature, °C	-146.36	-146.5	0.09
E1 Power, MW	1.74	1.69	2.87
Power consumed by C1, MW	57.23	58.47	2.16
Power consumed by C2, MW	18.53	18.42	0.59
Power consumed by C3, MW	29.04	27.075	6.77
Net power input, MW	102.35	101.41	0.92
Coefficient of performance (COP)	2.66	2.46	0.20
Exergy destruction, MW	40.95	40.21	1.81
Exergy efficiency, η_{ex} (%)	59.99	60.34	0.58

compressors is about 101.84 MW and 1.17 MW for the two expanders. The optimal COP and exergy efficiency of the cycle are 2.70 and 62.26% respectively in Table. 9.

From the results reported in Table 8 and Table 9, it can be deduced that the optimization allowed a decrease in the power consumed by the compressors of 2.82%, a decrease in the exergy destruction of the cycle of 7.23%; an improvement of the COP and exergy efficiency of 1.48% and 3.64% respectively compared to the basic cycle.

Table 9. Summary of optimal cycle performances

Parameter	Value
Expander output power MR, MW	0.70
Expander output power LNG, MW	0.47
Power consumed by C1, MW	56.54
Power consumed by C2, MW	17.63
Power consumed by C3, MW	27.67
Net power input, MW	100.67
Coefficient of performance (COP)	2.70
Exergy destruction, MW	37.99
Exergy efficiency, η_{ex} (%)	62.26

The results of the APCI cycle performance optimization obtained during this study are shown in Table 10 and compared with those of the literature.

It is seen that the results are in agreement with previously published studies; they show a gain in compressor power consumption, a decrease in exergy losses and an improvement in the COP and exergy efficiency of the basic cycle studied. The differences between the recorded performances are due to the difference between the parameters of the operating conditions of these cycles (temperature, pressure, flow rate, chemical composition of MR and NG).

The enhancement of the COP and exergy efficiency will result in a considerable reduction in NG consumption of the APCI process, hence an economic gain for the LNG Skikda Company.

Table 10. Comparison of APCI cycle optimization results with the literature

Performances APCI cycle	Abbasi Nezhad, S., et al. 2012 [38]	Mehrpooya & Ansarinasab 2015 [8]	Basic cycle APCI Skikda 2022	Optimized cycle APCI Skikda 2022
Compressor power, MW	42.72	130.75	104.80	101.84
Coefficient of performance (COP)	1.795	2.66	2.66	2.70
Exergy destruction, MW	26.26	72	40.95	37.99
Exergy efficiency, η_{ex} (%)	37.38	45	59.99	62.26

Finally, the results obtained for the performances of the cycle APCI Skikda are in good agreement with the literature.

CONCLUSIONS

The mixed refrigeration cycle of the LNG- APCI Skikda process was thermodynamically studied. The results of the energy analysis showed that the net power of the basic APCI cycle is about 102.35 MW and its COP is 2.66.

Exergy analysis pinpointed components whose irreversibility is high. The results of the exergy analysis showed that the total exergy destruction of the cycle is approximately 41 MW and its exergy efficiency is 60%. Compressors are the main energy consumer in the APCI process; they occupy with chillers the highest rate of the total exergy destruction 30.43% and 22.17% respectively.

The reduction of their exergy losses can be achieved by an adequate choice of the compression ratio as well as the inlet temperature.

In order to increase the performance of the APCI cycle, some key parameters have been analyzed. The results of the numerical simulation show that the compressor and expander inlet temperature as well as the NG temperature after cooling in the MCHE affect the COP and the exergy efficiency of the APCI cycle. COP and exergy efficiency will increase with decreasing compressor and expander inlet temperature and likewise with decreasing MCHE NG outlet temperature.

To improve the performance of the basic cycle, an optimization was carried. The GA was used as an optimization method considering the net energy consumption as an objective function for the cycle optimization.

The optimization results indicate that the power consumed by the compressors is reduced by 2.82% and the exergy destruction of the cycle by 7.23%. The optimal COP and exergy efficiency of the cycle are 2.70 and 62.26% respectively. They are improved by 1.48% and 3.64% respectively.

NOMENCLATURE

Ex	Specific exergy, kJ/kg
$\dot{E}x$	Exergy, MW
h	Enthalpy, kJ/kg
h'	Enthalpy at constant entropy, kJ/kg
$\dot{m}$	Flow rate, kg/s
P	Pressure, bar
$\dot{Q}$	Rate of heat flow, MW
s	Entropy, kJ/kg. K
T	Temperature, K
$\dot{W}$	Power, MW
x	Vapor fraction

Greek symbols

η_c	Compressor isentropic efficiency
η_{ex}	Exergy efficiency
η_j	Expander isentropic efficiency
$\Delta\dot{E}_{xd}$	Exergy destruction

Subscripts

c	Cold stream
h	Hot stream
in	Inlet
out	Outlet

Abbreviations

APCI	Air Products and Chemicals Inc
C	Compressor
C3MR	Propane pre-cooled mixed refrigerant
COP	Coefficient of performance
KBO	Knowledge Based Optimization
LNG	Liquefied Natural Gas
MCHE	Main Cryogenic Heat Exchanger
MR	Mixed Refrigerant
NG	Natural Gas
SMR	Single Mixed Refrigerant

AUTHORSHIP CONTRIBUTIONS

Authors equally contributed to this work.

DATA AVAILABILITY STATEMENT

The authors confirm that the data that supports the findings of this study are available within the article. Raw data that support the finding of this study are available from the corresponding author, upon reasonable request.

CONFLICT OF INTEREST

The author declared no potential conflicts of interest with respect to the research, authorship, and/or publication of this article.

ETHICS

There are no ethical issues with the publication of this manuscript.

REFERENCES

[1] He T, Karimi IA, Ju Y. Review on the design and optimization of natural gas liquefaction processes for onshore and offshore applications. Chem Eng Res Des 2018;132:89−114. [CrossRef]

[2] Kikkawa Y, Nakamura M, Sujiyama S. Development of liquefaction process for natural gas. J Chem Eng Japan 1997;30:625−630. [CrossRef]

[3] Cao WS, Lu XS, Li WS, Gu AZ. Parameter comparison of two small- scale natural gas liquefaction processes in skid-mounted packages. Appl Therm Eng 2006;26:898−904. [CrossRef]

[4] Vatani A, Mehrpooya M, Tirandazi B. A novel process configuration for co-production of NGL and LNG with low energy requirement. Chem Eng Process Process Intensif 2013;63:16−24. [CrossRef]
[5] Wang M., Khalilpour R, Abbas A. Operation optimization of propane precooled mixed refrigerant processes. J Nat Gas Sci Eng 2013;15:93−105. [CrossRef]
[6] Khan MS, Lee M. Design optimization of single mixed refrigerant natural gas liquefaction process using the particle swarm paradigm with nonlinear constraints. Energy 2013;49:146−155. [CrossRef]
[7] Kumar D, Mishra RS.Thermal analysis of cryogenic systems for liquefaction of various gases. International J Appl Eng Res 2014;9:3755−3780.
[8] Mehrpooya M, Ansarinasab H. Exergoeconomic evaluation of single mixed refrigerant natural gas liquefaction processes. Energy Convers Manag 2015;99:400−413. [CrossRef]
[9] Derbal C, Haouam A, Mzad H. Energy efficiency enhancement of mixed refrigerant process in LNG plant. Energy Procedia 2018;153:154−160. [CrossRef]
[10] Wang Q, Song Q, Zhang J, Liu R, Zhang S, Chen G. Experimental studies on a natural gas liquefaction process operating with mixed refrigerants and a rectifying column. Cryogenics 2019;99:7−17. [CrossRef]
[11] Hajji A, Chahartaghi M, Kahani M. Thermodynamic analysis of natural gas liquefaction process with propane pre-cooled mixed refrigerant process (C3MR). Cryogenics 2019;103:102978. [CrossRef]
[12] He T, Mao N, Liu Z, Qyyum MA, Lee M, Pravez AM. Impact of mixed refrigerant selection on energy and exergy performance of natural gas liquefaction processes. Energy 2020;199:117378. [CrossRef]
[13] Dokandari DA, Khoshkhoo RH, Bidi M, Mafi M. Thermodynamic investigation and optimization of two novel combined power-refrigeration cycles using cryogenic LNG energy. Int J Refrig 2021;124:167−183. [CrossRef]
[14] Rehman A, Qyyum MA, Qadeer K, Zakir F, He X, Nawaz A, et al. Single mixed refrigerant LNG process: Investigation of improvement potential, operational optimization, and real potential for further improvements. J Clean Prod 202;284:125379. [CrossRef]
[15] Alabdulkarem A, Mortazavi A, Hwang Y, Radermacher R, Rogers P. Optimization of propane pre-cooled mixed refrigerant LNG plant. Appl Therm Eng 2011;31:1091−1098. [CrossRef]
[16] Xu X, Liu J, Cao L. Optimization and analysis of mixed refrigerant composition for the PRICO natural gas liquefaction process. Cryogenics 2014;59:60−69. [CrossRef]
[17] Moein P, Sarmad M, Ebrahimi H, Zare M, Pakseresh S, Vakili SZ. APCI-LNG single mixed refrigerant process for natural gas liquefaction cycle: analysis and optimization. J Nat Gas Sci Eng 2015;26:470−479. [CrossRef]
[18] Nikkho S, Abbasi M, Zahirifar J, Saedi M, Vatani A. Energy and exergy investigation of two modified single mixed refrigerant processes for natural gas liquefaction. Comput Chem Eng 2020;140:106854. [CrossRef]
[19] Sayyaadi H, Babaelahi M. Exergetic optimization of a refrigeration cycle for re-liquefaction of LNG boil-off gas. Int J Thermodyn 2010;13:127−133.
[20] Kotas TJ. The exergy method of thermal plant analysis. Malabar, ABD: Krieger Publishing; 1995.
[21] Kabul A, Kizilkan O, Yakut AK. Performance and exergetic analysis of vapor compression refrigeration system with an internal heat exchanger using a hydrocarbon, isobutane (R600a). Int J Energy Res 2008;32:824−836. [CrossRef]
[22] Morosuk T, Tsatsaronis G, Schult M. Conventional and advanced exergetic analyses: theory and application. Arabian J Sci Eng 2013;38:395−404. [CrossRef]
[23] Venkatarathnam G. Cryogenic mixed refrigerant processes. 1st ed. New York: Springer; 2008. [CrossRef]
[24] Vatani A, Mehrpooya M, Palizdar A. Advanced exergetic analysis of five natural gas liquefaction processes. Energy Convers Manag 2014;78:720−737. [CrossRef]
[25] Palizdar A, Sadrameli SM. Conventional and advanced exergoeconomic analyses applied to ethylene refrigeration system of an existing olefin plant. Energy Convers Manag 2017;138:474−485. [CrossRef]
[26] Direk M, Mert MS, Soylu E, Yüksel F. Experimental investigation of an automotive air conditioning system using R444A and R152a refrigerants as alternatives of R134a. J Mech Eng 2019;65:212−218. [CrossRef]
[27] Mert MS, Dılmac OF, Ozkan S, Karaca F, Bolat E. Exergoeconomic analysis of a cogeneration plant in an iron and steel factory. Energy 2012;46:78−84. [CrossRef]
[28] Holland JH. Adaptation in natural and artificial systems: an introductory analysis with applications to biology, control, and artificial intelligence. Cambridge: MIT Press; 1992. [CrossRef]
[29] Whitley D. A genetic algorithm tutorial. Stat Comput 1994;4:65−85. [CrossRef]
[30] Mitchell M. An introduction to genetic algorithms. Reprint ed. Cambridge: MIT Press; 1998.
[31] He T, Ju Y. Design and optimization of a novel mixed refrigerant cycle integrated with NGL recovery process for small-scale LNG plant. Ind Eng Chem Res 2014;53:5545−5553. [CrossRef]
[32] Khan MS, Lee S, Lee M. Optimization of single mixed refrigerant natural gas liquefaction plant with nonlinear programming. Asia-Pac J Chem Eng 2012;7:62−70. [CrossRef]
[33] Qyyum MA, Qadeer K, Lee S, Lee M. Innovative propane-nitrogen two-phase expander refrigeration cycle for energy-efficient and low-global warming potential LNG production. Appl Therm Eng 2018;139:157−165. [CrossRef]

[34] Zhu J, Zhang W, Liu S, Li Y, Liu M, Yin Q, Li Y. Experiment and dynamic simulation study on propane pre-cooling double nitrogen-expander liquefaction process for medium-pilot LNG plant. Appl Therm Eng 2020;170:114994. [CrossRef]
[35] Li QY, Ju Y. Design and analysis of liquefaction process for offshore associated gas resources. Appl Therm Eng 2010;30:2518−2525. [CrossRef]
[36] Yuan Z, Cui M, Xie Y, Li C. Design and analysis of a small-scale natural gas liquefaction process adopting single nitrogen expansion with carbon dioxide pre-cooling. Appl Therm Eng 2014;64:139-146. [CrossRef]
[37] He T, Ju Y. Optimal synthesis of expansion liquefaction cycle for distributed-scale LNG (liquefied natural gas) plant. Energy 2015;88:268−280. [CrossRef]
[38] Nezhad SA, Shabani B, Soleimahadni M. Thermodynamic analysis of liquefied natural gas (LNG) production cycle in APCI process. J Therm Sci 2012; 21:564−571. [CrossRef]

Appendix 1.

The thermodynamic properties at each point in the MR cycle of the APCI process are given in Appendix 1.

Appendix 1. The stream parameters of the basic APCI cycle.

Stream N°	*T* (°C)	*P* (bar)	*in* (kg/s)	*h* (kJ/kg)	*s* (kJ/kg.K)	*Ex* (kJ/kg)	"x"
1	22.46	63	233.39	-3857	7.727	532.022	1
2	-5.13	62.52	233.39	-3931	7.466	535.53	0.99
3	-22.17	62.04	233.39	-3986	7.255	542.63	0.97
4	-35.15	61.56	233.39	-4034	7.060	552.50	0.95
5	-39.90	60.67	233.78	-4150	7.434	581.62	1
6	-38.99	60.67	236.92	-4129	7.362	575.64	0.99
7	-55.33	56.19	236.92	-4195	7.089	592.66	0.91
8	-55.33	56.19	31.99	-3889	4.581	611.97	0.02
9	-55.33	56.19	204.86	-4244	7.461	612.22	1
10	-53.66	61.89	31.99	-3887	4.586	530.51	1
11	82.22	60.72	31.60	-2624	3.218	257.89	0
12	-39.17	4.3	359.039	-3295	6.996	161.23	1
13	62.43	21.16	359.039	-3127	7.075	314.13	1
14	34.16	20.61	359.039	-3185	6.901	307.12	1
15	66.48	32.35	359.039	-3133	6.926	358.62	1
16	34.72	31.80	359.039	-3202	6.717	351.34	1
17	85.88	63.09	359.039	-3124	6.750	434.42	1
18	40.76	62.60	359.039	-3239	6.410	421.06	1
19	40.76	62.60	232.34	-3239	6.410	421.06	1
20	13.50	62.25	232.34	-3319	6.145	420.18	1
21	-5.13	61.90	232.34	-3426	5.758	425.22	0.71
22	-22.17	61.55	232.34	-3530	5.357	434.56	0.38
23	-35.15	61.20	232.34	-3602	5.065	444.71	0.17
24	40.76	62.60	126.52	-3239	6.410	421.06	1
25	19.24	61.95	126.52	-3300	6.213	419.09	1
26	-0.20	61.30	126.52	-3391	5.890	422.17	0.82
27	-18.27	60.65	126.52	-3505	5.459	430.18	0.47
28	-35.71	60	126.52	-3602	5.066	442.86	0.18
29	-35.69	60	358.86	-3602	5.066	442.84	0.18
30	-35.69	60	303.41	-3614	4.747	427.96	0

Stream N°	*T* (°C)	*P* (bar)	*in* (kg/s)	*h* (kJ/kg)	*s* (kJ/kg.K)	*Ex* (kJ/kg)	"x"
31	-128.94	49.66	303.41	-3899	3.534	533.68	0
32	-129.3	12.68	3303.41	-3904	3.544	402.09	0
33	-134.14	4.70	303.41	-3885	3.385	312.77	0.06
34	-35.69	60	44.35	-3539	6.804	522.15	1
35	-145.94	59.50	44.35	-4044	4.104	728.28	0
36	-152.30	4.90	44.35	-4043	4.198	440.16	0.1
37	-35.69	60	11.095	-3539	6.804	522.15	1
38	-161.72	59.66	11.095	-4087	3.740	785.97	0
39	-159.97	4.90	11.095	-4088	3.819	478.76	0
40	-153.79	4.90	55.45	-4052	4.123	447.25	0.08
41	-35.71	64.50	1.10	-2598	0.148	156.50	0
42	-31.70	65.50	3.14	-2709	0.717	190.47	0
43	-35.71	64.50	1.10	-2598	0.148	156.48	0
44	-145.94	45.85	205.96	-4732	4.686	790.29	0
45	-146.36	21.79	205.96	-4735	4.695	693.09	0
46	-147.77	5.40	5.61	-2017	6.180	340.16	1
47	-37.91	5.19	5.61	-1848	7.167	210.11	1
48	-147.77	5.40	200.35	-4808	4.682	508.95	0
49	-153.12	4.92	200.35	-4826	4.541	515.59	0
50	-162.74	1.36	179.53	-5125	4.344	385.05	0
51	-160.55	1.34	179.53	-5104	4.533	368.10	0.03
52	-163.94	1.26	26.68	-2467	6.789	197.57	0.99
53	-37.91	1.05	26.68	-2274	8.036	16.25	1
54	-160.55	1.34	173.66	-5165	4.424	373.23	0
55	-160.35	7.01	173.66	-5166	4.413	605.77	0